Title
Modified Method of Characteristics for Transient Radiative Transfer

Journal
Journal of Quantitative Spectroscopy and Radiative Transfer, 98(2)

Authors
Katika, Kamal M.
Pilon, Laurent

Publication Date
2006

Peer reviewed

Modified Method of Characteristics in Transient Radiation Transfer

Kamal M. Katika and Laurent Pilon

Mechanical and Aerospace Engineering Department

Henri Samueli School of Engineering and Applied Science

University of California, Los Angeles - Los Angeles, CA 90095, USA

Phone: +1 (310)-206-5598, Fax: +1 (310)-206-2302

E-mail: pilon@seas.ucla.edu

June 15, 2005

Abstract

This paper presents the modified method of characteristics for simulating multidimensional transient radiative heat transfer in emitting, absorbing and scattering media. The method is based on the method of characteristics that follows photons along their pathlines. It makes use of a fixed set of points, and unlike the conventional method of characteristics, it follows the photons backward in space. Test problems involving diffuse irradiation in 1-D and 3-D participating media and collimated irradiation in 1-D participating media were considered. The results show good agreement with analytical and numerical solutions reported in literature. The scheme is fast and was able to capture the sharp discontinuities associated with the propagation of a radiation front in transient radiation transport.

Keywords: transient radiative transfer, method of characteristics, scattering, turbid media, tomography, biological tissues

NOMENCLATURE

c	speed of light in vacuum $= 2.998 \times 10^8 m/s$
g	scattering anisotropy factor in the Henyey-Greenstein phase function
I	radiation intensity
L	length
N_x	number of nodes in the x-direction
N_y	number of nodes in the y-direction
N_z	number of nodes in the z-direction
N_θ	number of discrete polar angles for θ varying from 0 to π
N_ϕ	number of discrete azimuthal angles for ϕ varying from 0 to 2π
$\mathbf{q}$	heat flux
s	geometric path length
S	source term in the radiative transfer equation
t	time
t_c	time at which the peak of an ultra-short pulse occurs
t_p	pulse width
Δt	time step
$\hat{\mathbf{s}}$	direction unit vector
x, y, z	Cartesian coordinates
Δz	element size along z axis

Greek symbols

β	extinction coefficient $(= \sigma_s + \kappa)$

θ	polar angle
κ	absorption coefficient
λ	wavelength
μ	direction cosine ($= \cos\theta$)
σ	Stefan-Boltzman constant $= 5.67 \times 10^{-8} W/m^2K^4$
σ_s	Scattering coefficient
τ	optical distance ($= \int_0^z \beta \mathrm{d}z$)
ϕ	azimuthal angle
Φ	scattering phase function
ω	scattering albedo ($= \sigma_s/\beta$)
Ω	solid angle

Subscripts

b	refers to blackbody behavior
c	refers to collimated intensity
d	refers to diffuse intensity
L	value at location z = L
w	value at the boundary
λ	at a given wavelength λ, or per unit wavelength

1 INTRODUCTION

Traditional analysis of radiation transfer neglects the transient effect of light propagation due to the large speed of light compared to the local time and length scales [1]. Of late, with the advent of ultra-short pulsed lasers, this assumption is no longer valid as the temporal width of the input pulse is similar to the order of the radiation propagation time in the system and usually of the order of pico- and femto- seconds. Ultra-short pulsed lasers are used in a wide variety of applications such as thin film property measurements, laser assisted micro-machining, laser removal of contamination particles from surfaces, optical data storage, optical ablation and ablation of polymers [2]. Ultra-short pulsed lasers are also used in remote sensing of the atmosphere, combustion chambers and other environments which involve interaction of the laser beam with scattering and absorbing particles of different sizes. Particle size distributions and their optical properties can be reconstructed from measuring transmitted and reflected signals from short-pulsed lasers [2]. Another interesting application of short-pulsed lasers is in biomedical optical tomography where their use can potentially provide physiological and morphological information about the interior of living tissues and organs in a non-intrusive manner. Yamada [3] has described a technique to compute the properties of a tissue based on temporal intensity measurements and an inverse method in order to determine the health of the tissue [3].

All the applications described above require models to predict transient radiation transport in participating media. In the past, various analytical studies and numerical models of transient radiative transfer have been reviewed by Mitra and Kumar [4]. They examined the transport of light pulses through absorbing-scattering media with different approximate

mathematical models. They have shown that the propagation speed of scattered radiation, the magnitudes of the transmitted and backscattered fluxes and the temporal shape of the optical signals are dependent on the model used. This is because, the speeds of propagation are obtained by averaging over different lines of sight oriented at different angles from the primary direction of propagation [4]. The diffusion approximation has been extensively used in biomedical applications [5,6] in order to simplify the radiative transfer problem. However, its validity for transient light transport in heterogeneous biological tissues with nonscattering or low-scattering regions has been questioned [7]. Indeed, Elaloufi *et al.* [7] have shown that the diffusion approximation fails to describe both short-time and long-time radiation transport in optically thin slabs. In the case of optically thick slabs, the diffusion approximation fails for short times. The authors have also shown that the diffusion theory always fails to predict the long-time behavior of transmitted pulses in thin slabs whose optical depth, defined by $\tau_L = \sigma_s(1-g)L$, is less than eight. This issue has also been discussed by Guo and Kim [8] in the transport of ultra-fast laser pulses in biological tissues. As a result, alternatives to the diffusion approximation need to be formulated for accurately predicting transient transport in optically thin and heterogeneous media.

The governing equation for radiation transfer in a participating medium is the radiative transfer equation (RTE). The RTE expresses an energy balance in a unit solid angle of $d\Omega$ about the direction $\hat{\mathbf{s}}$ within a wavelength interval $\mathrm{d}\lambda$ about λ. It can be written as [1],

$$\frac{1}{c}\frac{\partial I_\lambda}{\partial t} + (\hat{\mathbf{s}}\cdot\nabla)I_\lambda = \kappa_\lambda I_{b\lambda} - \kappa_\lambda I_\lambda - \sigma_{s\lambda} I_\lambda + \frac{\sigma_{s\lambda}}{4\pi}\int_{4\pi} I_\lambda(\hat{\mathbf{s}}_i)\Phi_\lambda(\hat{\mathbf{s}}_i,\hat{\mathbf{s}})\mathrm{d}\Omega_i \qquad (1)$$

where I_λ is the intensity in the $\hat{\mathbf{s}}$ direction and c, the speed of light in the medium. The linear absorption and scattering coefficients are denoted by κ_λ and $\sigma_{s\lambda}$, respectively. The

first term on the right-hand side represents the contribution from emission in the $\hat{\mathbf{s}}$ direction; the second and third terms represent attenuation by absorption and scattering, respectively. Finally, the last term on the right hand side corresponds to the augmentation of radiation due to in-scattering. The scattering phase function $\Phi_\lambda(\hat{\mathbf{s}}_i, \hat{\mathbf{s}})$ represents the probability that radiation propagating in the solid angle $\mathrm{d}\Omega_i$ direction around $\hat{\mathbf{s}}_i$ be scattered into the cone $\mathrm{d}\Omega$ around the direction $\hat{\mathbf{s}}$.

As can be seen from Equation (1), the RTE is an integro-differential equation involving seven independent variables: (i) the wavelength of radiation λ, (ii) three space coordinates x, y, and z, (iii) two coordinates describing the direction of travel, polar angle θ and azimuthal angle ϕ, and (iv) time t. Various other factors like geometry, temperature fields, and the radiation characteristics of the medium make radiative transfer problems difficult to solve. The analysis is further complicated by the fact that radiation characteristics $\sigma_{s\lambda}$, κ_λ, and Φ_λ of materials may depend on wavelength, temperature, and location. Moreover, they are difficult to measure and often display irregular behavior [1]. Because of the nature of the radiative transfer equation and various effects described above, exact solutions of the RTE are difficult and exact analytical solutions exist for only a few simple cases [1].

The commonly used methods to solve the transient radiative transfer equation are the Monte Carlo method, the integral equation solution, the finite volume method (FVM), the radiation element method (REM), and the discrete ordinates method (DOM).

The Monte Carlo method is often used to simulate problems involving radiative heat transfer because of its simplicity, the ease by which it can be applied to arbitrary configurations and its ability to capture actual and often complex physical conditions [9]. The Monte Carlo technique has been used by Guo *et al.* [9] to simulate short-pulsed laser transport

in anisotropically scattering and absorbing media. The authors studied the effects of pulse width, medium properties, and the effects of Fresnel reflection on the transmissivity and reflectivity of the medium. The Monte Carlo method has also been widely used in biomedical optics to simulate steady-state laser transport in biological tissue [10]. Jacques used a Monte Carlo model to simulate the propagation of femtosecond and picosecond laser pulses within turbid tissues [11]. However, the method has inherent statistical errors due to its stochastic nature [1]. It is also computationally time consuming and demands a lot of computer memory as the histories of the photons have to be stored at every instant of time [9]. Thus, the Monte-Carlo method is ruled out in practical utilizations such as real-time clinical diagnostics where computational efficiency and accuracy are major concerns [12].

The backward or reverse Monte Carlo has been developed as an alternative approach when solutions are needed only at particular locations and times [13, 14]. The method is similar to the traditional Monte Carlo method, except that the photons are tracked in a time-reversal manner. The photon bundles are traced backward from the detector to the source rather than forward from the source to the detector as in the conventional Monte Carlo method. There is no need to keep track of photons which do not reach the detector and so the reverse Monte Carlo method is much faster than the traditional Monte Carlo method [13]. The method was successfully applied by Lu and Hsu [14] to simulate transient radiative transport in a non-emitting, absorbing, and anisotropically scattering one-dimensional slab subjected to ultra-short light pulse irradiation.

Analytical solutions of the radiation transfer equation in integral form for inhomogeneous and non-scattering medium have been obtained by Pomraning [15] and Munier [16–19]. Wu and co-workers [20, 21] and Tan and Hsu [22] have also used the integral equation formula-

tion to solve the transient radiative transfer problem. Wu [20] used the integral equation to compute the temporal reflectivity and transmissivity of 1-D absorbing and isotropically scattering slabs with various scattering albedos and optical thicknesses which compared well with results obtained using the Monte Carlo method. Tan and Hsu [22] used the formulation to simulate radiative transport in 1-D absorbing and isotropically scattering media with black boundaries exposed to diffuse or collimated irradiation. The authors extended the method to solve the same problem in 3-D geometries [23].

Finite volume methods developed by Raithby and Chui [24] to solve the steady-state RTE have also been employed by Chai and co-workers [25, 26] to solve the transient RTE. They used the finite volume technique with the "step" and CLAM spatial discretization schemes to model transient radiative transfer in 1-D and 3-D geometries [25, 26]. The authors found that the CLAM scheme captures the penetration depths of radiation more accurately than the "step" scheme for the same grid.

Moreover, Guo and Kumar [27] used the radiation element method to solve the transient RTE in 1-D absorbing and scattering media exposed to both diffuse and collimated irradiation.

Finally, the discrete ordinates method has been used by various researchers to solve the transient RTE. Sakami *et al.* [28] used the DOM to analyze the ultra-short light pulse propagation in an anisotropically scattering 2-D medium. Guo and Kumar [12] used it to simulate short-pulse laser transport in two-dimensional anisotropically scattering turbid media. They later extended the technique to solve for 3-D geometries and compared the results with Monte Carlo simulations [29]. They found that the transient discrete ordinates method cannot capture the abrupt changes in the transmittance as predicted by the Monte

Carlo method. Guo and Kim [8] further used the DOM in 3-D geometries to model ultrafast laser pulses in heterogeneous biological tissues for the purpose of detecting inhomogeneities in otherwise homogeneous tissue. Quan and Guo [30] also used the same technique to model transport of fluorescence in tissue to detect tumors.

This paper aims at presenting the modified method of characteristics as a means of solving the transient radiative transfer equation. First, a description of the method is given, followed by simulations of test cases for which exact and numerical solutions have been reported in the literature.

2 MODIFIED METHOD OF CHARACTERISTICS

The conventional method of characteristics (or direct marching method) is commonly used to solve hyperbolic partial differential equations which often occur in compressible fluid flow [31]. It is based on the Lagrangian formulation, which identifies photons or particles in general, at initial time $t = t_0$ and follows them along the characteristic at subsequent times as they are transported. Characteristics are pathlines of photons in physical space along which information propagates. Though the direct method results in accurate solutions, it has several disadvantages. Time increments along different characteristic curves may be different and so the solution may be obtained at different times on each characteristic curve. Also, the characteristic curves may coalesce or spread apart due to non-uniform velocities resulting in a highly distorted grid [31].

The modified method of characteristics on the other hand, follows photons backward in space and uses any arbitrary pre-specified set of points. Thus, the solution is obtained at

the same times at all points and overcomes the problems related to grid deformation [31,32]. The modified method of characteristics has been successfully used for predicting high speed three-dimensional single phase inviscid flows in subsonic and supersonic propulsion nozzles [33, 34] and combined with the finite element method for solving unsteady incompressible Navier-Stokes equations [32]. Recently, Pilon and co-workers used the modified method of characteristics to solve the population balance equation for bubbles and solid particles [35–37] as well as for phonons [38].

The present study aims at applying the modified method of characteristics to the transient radiative transfer equation. Consider a Cartesian coordinate system, the characteristic curve in physical space is defined by

$$\frac{\mathrm{d}x}{\mathrm{d}t} = c\sin\theta\cos\phi \tag{2}$$

$$\frac{\mathrm{d}y}{\mathrm{d}t} = c\sin\theta\sin\phi \tag{3}$$

$$\frac{\mathrm{d}z}{\mathrm{d}t} = c\cos\theta \tag{4}$$

By definition, the total derivative of $I_\lambda(x, y, z, t)$ can be written as

$$\frac{\mathrm{D}I_\lambda}{\mathrm{D}t} = \frac{\partial I_\lambda}{\partial t} + \frac{\mathrm{d}x}{\mathrm{d}t}\frac{\partial I_\lambda}{\partial x} + \frac{\mathrm{d}y}{\mathrm{d}t}\frac{\partial I_\lambda}{\partial y} + \frac{\mathrm{d}z}{\mathrm{d}t}\frac{\partial I_\lambda}{\partial z} \tag{5}$$

Then, along the characteristic curves in (x, y, z, t) space, the RTE [Equation (1)] simplifies to

$$\frac{1}{c}\frac{\mathrm{D}I_\lambda}{\mathrm{D}t} = -\kappa_\lambda I_\lambda - \sigma_{s\lambda} I_\lambda + \kappa_\lambda I_{b\lambda} + \frac{\sigma_{s\lambda}}{4\pi}\int_{4\pi} I_\lambda(\hat{\mathbf{s}}_i)\Phi_\lambda(\hat{\mathbf{s}}_i, \hat{\mathbf{s}})\mathrm{d}\Omega_i \tag{6}$$

Thus, the spatio-temporal partial integro-differential Equation (1) is converted into 3 ordinary differential equations in time, [Equations (2) to (4)] and 1 temporal integro-differential equation [Equation (6)]. Figure 1 shows a 3-D computational cell in Cartesian coordinates.

The modified method of characteristics consists of determining the coordinates (x_n, y_n, z_n) of the point in space from where the particles located at the grid point (x_a, y_b, z_c) at time $t + \Delta t$ originate from at time t while travelling in direction of polar angle θ_n and azimuthal angle ϕ_m. In other words, for each point of a specified grid, the pathline is projected rearward along the characteristic curve to the initial data surface to determine the initial data point. For example, in Figure 1, the point (x_a, y_b, z_c) is the point $(x_{i+1}, y_{j+1}, z_{k+1})$. The solid line represents the section of the characteristic curve along which the photon traveled from location (x_n, y_n, z_n) to location (x_a, y_b, z_c) during the time interval between t and $t+\Delta t$. The general block diagrams of the numerical procedures for solving the RTE using the modified method of characteristics is shown in Figure 2.

To solve Equations (2) to (6), the radiation intensities and temperatures are initialized at all points in the computational domain. Then, for a given polar angle θ_n, an azimuthal angle ϕ_l, and for all internal grid points (x_a,y_b,z_c) where photons are present at time $t + \Delta t$, the position of the photon at time t is calculated as

$$x_n = x_a - c \sin\theta_n \cos\phi_l \Delta t \tag{7}$$

$$y_n = y_b - c \sin\theta_n \sin\phi_l \Delta t \tag{8}$$

$$z_n = z_c - c \cos\theta_n \Delta t \tag{9}$$

The values of the variables I_λ at (x_n, y_n, z_n) and time t are obtained by Lagrangian interpolation using their values at time t at the eight corners of the computational cell in which the point (x_n, y_n, z_n) is located (Figure 1). Then, Equation (6) is solved forward in time by the fourth order Runge-Kutta method at location (x_a, y_b, z_c) and time $t + \Delta t$. The integral on the right hand side of Equation (6) is estimated by the 3/8 Simpson numerical integration

with intensity values at time t. Finally, the boundary conditions are imposed in directions pointing toward the medium depending on whether the boundary is black, specularly or diffusely reflecting. For directions leaving the computational domain (outflow), the intensities at the boundary are computed just like any other internal point. The calculations are repeated for all the discretized values of polar and azimuthal angles.

The modified method of characteristics has the following main advantages:

- Unlike finite volume techniques which propagate the information along the coordinate axis, the modified method of characteristics propagates information along the photon pathlines. Like the Monte Carlo method, it respects the physics of radiative transport resulting in accurate numerical results.

- Since the method uses any arbitrary pre-specified set of points, it can be easily coupled with other numerical techniques such as finite volume, finite element or finite difference schemes. This is a valuable feature in situations involving multiple transport processes, for example, ultra-short pulse laser heating of metals [39].

- It does not require any outflow boundary conditions. The radiative transport equation is a hyperbolic equation and information propagates with finite speed, *i.e.*, the speed of light in the medium. In such equations, the solution at a point is determined only by the characteristics from the upstream portion of the solution domain [31].

There are also a few disadvantages in using the modified method of characteristics to solve the RTE. The backward projected characteristic curves do not necessarily intersect the known solution surface at the pre-specified grid points and so the initial data at the backward

projected characteristics must be determined by interpolation. This takes up computational effort and introduces interpolation errors into the solution.

The method described above could be considered as a hybrid method between the traditional discrete ordinates and the ray tracing methods. It is similar to the discrete ordinates method in that the RTE is solved along arbitrary directions. However, the modified method of characteristics converts the RTE into ordinary differential equations in time and solved along the characteristics, as opposed to the conventional implementation of the DOM [1], where the RTE in the form of a partial differential equation is solved along the grid lines. The present approach is comparable to that used by Coelho [40] to solve the RTE using the discrete ordinates method. The author determined the dependent variable I_λ by the values at points located at the intersection of the direction of propagation of radiation with the grid lines or surfaces, as opposed to directly using the grid nodes in the conventional DOM. The present method also differs from that used by Coelho in the sense that, the photons are traced back a distance which they would travel in one time step rather than all the way to the grid lines or surfaces.

Finally, unlike ray-tracing methods, the modified method of characteristics does not trace photon bundles from the source to the absorption point or to the boundaries. Instead photon bundles are traced backward in space only for the time interval between t and $t + \Delta t$. At a new time step, new photon bundles are traced back from all grid points and this procedure is repeated for all time steps.

3 RESULTS AND DISCUSSION

For validation purposes, the numerical results obtained with the modified method of characteristics for a set of test cases have been compared with analytical solutions or numerical results reported in the literature using different numerical schemes. For the sake of clarity, spectral dependencies were not considered in these cases but could have been included without any modifications in the methodology. The spectral dependencies can be accounted for by using the modified method of characteristics at multiple wavelengths or in combination with band models [1]. The test cases considered consist of simulations of transient radiation transfer in absorbing and isotropically scattering cold media namely, (1) a plane parallel slab exposed to diffuse irradiation, (2) three-dimensional media exposed to diffuse irradiation, (3) a plane parallel slab irradiated by continuous collimated radiation, (4) and a plane parallel slab irradiated by pulsed collimated radiation.

For 1-D problems, a discretization of N_z points along the $z-$direction and N_θ discrete directions for θ varying from 0 to π was used. In the case of 3-D problems, a discretization of $N_x \times N_y \times N_z$ along the x, y and $z-$directions respectively was used and the angular space of θ varying from 0 to π and ϕ varying from 0 to 2π was discretized into $N_\theta \times N_\phi$ directions.

3.1 1-D transient radiative transfer in scattering, absorbing, and emitting media exposed to diffuse irradiation

Let us consider the case of a plane-parallel slab of a non-emitting, absorbing and isotropically scattering medium of thickness L. It is subjected to a transient unit step function emissive power on one side ($z = 0$) and the other side ($z = L$) is cold. The slab's optical thickness

τ_L defined as $\tau_L = \int_0^L \beta \mathrm{d}z$ is equal to 1.0 where $\beta = \sigma_s + \kappa$ and the scattering albedo $\omega = \dfrac{\sigma_s}{\beta} = 0.5$. Initially, the medium is assumed to be at 0K and initial intensities everywhere in the medium are zero. Then, at t=0 a diffuse intensity $I(z = 0, \mu > 0, t) = 1.0\ W/m^2 sr$ is imposed. The time interval Δt is equal to $\Delta z/c$ where $\Delta z = L/100$. After solving for the intensities in all directions at every grid point, the heat flux can be calculated from

$$\mathbf{q} = \int_{4\pi} I(\hat{\mathbf{s}})\hat{\mathbf{s}}\mathrm{d}\Omega \tag{10}$$

Figure 3 compares the radiative flux distribution as a function of time obtained with the modified method of characteristics and the integral equation solution reported by Tan and Hsu [22]. A converged solution was obtained for a grid size $N_z = 101$ and $N_\theta = 25$ angular directions. The CPU time for this calculation on a Pentium 4, 2.80 GHz machine for 360 time steps was about 6 seconds. Note that Tan and Hsu [22] reported an execution time of about 1800 seconds on a Pentium-Pro 200 MHz PC with 100 elements and 400 time steps.

The error in the radiative flux computed by the present method with a grid size of $N_z = 101$ and $N_\theta = 25$ angles and that reported by Tan and Hsu [22] was less than 1.3% for all values of $t/\Delta t$ except at the radiation front where it went up to 3% for $t/\Delta t = 30$, 6% $t/\Delta t = 60$ and 10% at a single point for $t/\Delta t = 90$.

The same problem was solved by Chai [25] using the finite volume method. The author used two different spatial discretization schemes, namely the "step" and the CLAM scheme to solve the transient RTE with 300 control volumes and $N_\theta = 40$. The CLAM scheme resulted in better accuracies than the "step" scheme for the same grid size. According to the author, "both schemes predict the incident radiation and the radiative flux accurately once the radiation reaches the opposite side ($z/L = 1$) of the slab. For $t = \Delta t_c \leq 90$, the

step scheme overpredicts both the radiative flux and the incident radiation at the radiation front" [25]. On the other hand, the modified method of characteristics captures the radiation front accurately even for $t = \Delta t \leq 90$ and with fewer control volumes (see Figure 3).

3.2 3-D transient radiative transfer in scattering, absorbing, and emitting media exposed to diffuse irradiation

The same analysis done for the one-dimensional case can be extended to 3-D geometries and applied to a cubic enclosure with one hot wall. The optical thickness of the medium defined by $\tau_L = \beta L$ was set at 1.0 and the scattering albedo ω was 0.1. Initially, the medium is assumed to be at a temperature of 0K and initial intensities everywhere in the medium are zero. Then, at t=0, the intensity at the wall, $z = 0.0$ in all directions pointing into the medium is set to 1.0 W/m^2sr. The remaining walls are black and cold ($T = 0K$).

A grid size of $35 \times 35 \times 35$ points along the x, y and $z-$directions was used. The entire angular space of θ varying from 0 to π and ϕ varying from 0 to 2π was divided into 30×24 discrete directions. Tan and Hsu [23] solved the same problem using the integral solution. The authors verified the reliability of the integration scheme, namely the DRV method, by comparing their results with those obtained by using the YIX method. They used a grid size of $17 \times 17 \times 17$ volume elements in the x, y and $z-$directions respectively in all the cases and 1982 angular quadrature points for the YIX method. Similarly, Chai *et al.* [26] solved this problem using the finite volume method. Figure 4 compares the heat flux along the center of the cube obtained using the present method with those obtained by (i) Tan and Hsu [23] with the integral solution using the DRV scheme and (ii) Chai *et al.* [26] using a grid size

of $17 \times 17 \times 17$, an angular discretization of 16×12 and making use of the CLAM scheme. In order to quantify the relative difference in the numerical results, we assumed that the values reported by Tan and Hsu [23] are converged and correspond to the exact solution. For steady-state, the relative error for the results reported by Chai *et al.* [26] compared to Tan and Hsu [23] was less than 2.5% while they were less than 6% for the present method. For the intermediate transients, the results reported by Chai *et al.* [26] result in infinite errors beyond the wavefront. Chai *et al.* [26] found that the finite volume method suffers from false scattering and cannot capture the wavefront accurately. In contrast, the present method is able to accurately capture the wavefront. However, there were large errors of up to 83% at the point right before the wavefront. It was less than 6% at all other points. This could be attributed to the fact that the solution was not converged in terms of the grid size or the number of directions. In order to minimize the error, a further refinement in the grid size was attempted, but was out of bounds in terms of memory and processing power for the single processor computer used. It is anticipated that a refinement in grid size and directions will reduce the error.

3.3 1-D transient radiative transfer with collimated irradiation

To solve the radiative transport equation for collimated irradiation, the intensity is split into two parts, (i) the radiation scattered away from the collimated radiation and (ii) the remaining collimated beam after partial extinction by absorption and scattering along its path. The contribution from emission is usually negligible compared to the incident and

scattered intensity. Thus, the intensity for a gray medium is written as [1],

$$I(\mathbf{r}, \hat{\mathbf{s}}, t) = I_c(\mathbf{r}, \hat{\mathbf{s}}, t) + I_d(\mathbf{r}, \hat{\mathbf{s}}, t) \tag{11}$$

The incident irradiation is $I_i(\mathbf{r}_w, t)$, where $\mathbf{r}_w$ is the location on the bounding surface of the medium where the radiation is incident. The collimated intensity I_c, remnant of this incident irradiation, obeys the equation of transfer

$$\frac{1}{c}\frac{\partial I_c(\mathbf{r}, \hat{\mathbf{s}}, t)}{\partial t} + \hat{\mathbf{s}} \cdot \nabla I_c(\mathbf{r}, \hat{\mathbf{s}}, t) = -\beta I_c(\mathbf{r}, \hat{\mathbf{s}}, t) \tag{12}$$

subject to the boundary condition

$$I_c(\mathbf{r}_w, \hat{\mathbf{s}}, t) = I_i(\mathbf{r}_w, t)\delta[\hat{\mathbf{s}} - \hat{\mathbf{s}}_c(\mathbf{r}_w)] \tag{13}$$

The solution of these equations is given by [15],

$$I_c(\mathbf{r}, \hat{\mathbf{s}}, t) \;=\; I_i(\mathbf{r}_w, t - s/c)\delta[\hat{\mathbf{s}} - \hat{\mathbf{s}}_c(\mathbf{r}_w)] \times \exp\left[-\int_0^s \beta(\mathbf{r} - s'\hat{\mathbf{s}})ds'\right] H(t - s/c) \tag{14}$$

where $s = |\mathbf{r} - \mathbf{r}_w|$ and H is the Heaviside step function [$H(u) = 0$ if $u < 0$ and $H(u) = 1$ if $u \geq 0$]. Substituting Equations (11) and (12) into Equation (1) for a gray medium gives the governing equation for the noncollimated radiation intensity I_d,

$$\begin{aligned}\frac{1}{c}\frac{\partial I_d(\mathbf{r}, \hat{\mathbf{s}}, t)}{\partial t} + \hat{\mathbf{s}} \cdot \nabla I_d(\mathbf{r}, \hat{\mathbf{s}}, t) = -\beta(\mathbf{r}) I_d(\mathbf{r}, \hat{\mathbf{s}}, t) + \kappa(\mathbf{r}) I_b(\mathbf{r}, \hat{\mathbf{s}}, t) \\ + \frac{\sigma_s(\mathbf{r})}{4\pi}\int_{4\pi} I_d(\mathbf{r}, \hat{\mathbf{s}}_i, t)\Phi(\hat{\mathbf{s}}_i, \hat{\mathbf{s}})\mathrm{d}\Omega_i + \sigma_s(\mathbf{r}) S_c(\mathbf{r}, \hat{\mathbf{s}}, t)\end{aligned} \tag{15}$$

where $S_c(\mathbf{r}, \hat{\mathbf{s}}, t)$ is the source term given by

$$S_c(\mathbf{r}, \hat{\mathbf{s}}, t) = \frac{1}{4\pi}\int_{4\pi} I_c(\mathbf{r}, \hat{\mathbf{s}}_i, t)\Phi(\hat{\mathbf{s}}_i, \hat{\mathbf{s}})\mathrm{d}\Omega_i \tag{16}$$

Note that Equations (12) and (15) sum up to give Equation (1). Moreover, the heat flux is computed using

$$\mathbf{q} = \int_{4\pi} I_d(\hat{\mathbf{s}})\hat{\mathbf{s}}\mathrm{d}\Omega + I_i(\mathbf{r}_w, t - s/c)\exp\left[-\int_0^s \beta(\mathbf{r} - s'\hat{\mathbf{s}}_c)ds'\right] H(t - s/c)\hat{\mathbf{s}}_c \tag{17}$$

Consider a plane parallel slab of an absorbing and isotropically scattering medium with constant and uniform optical properties exposed to time-dependent collimated radiation. In this case, Equation (14) simplifies to

$$I_c(z, \hat{\mathbf{s}}, t) = I_i(t - z/c)\delta[\hat{\mathbf{s}} - \hat{\mathbf{s}}_c]e^{-\beta z} \tag{18}$$

where $\hat{\mathbf{s}}_c$ corresponds to $\cos\theta = 1$. Moreover, the source term defined in Equation (16) simplifies to

$$S_c(z, t) = \frac{1}{4\pi} I_i(t - z/c)e^{-\beta z}H(t - z/c) \tag{19}$$

Equation (6) then becomes

$$\frac{1}{c}\frac{\mathrm{D}I_d(z, \hat{\mathbf{s}}, t)}{\mathrm{D}t} = -\beta I_d(z, \hat{\mathbf{s}}, t) + \frac{\sigma_s}{4\pi}\int_{4\pi} I_d(z, \hat{\mathbf{s}}_i, t)\mathrm{d}\Omega_i + \frac{\sigma_s}{4\pi} I_i(t - z/c)e^{-\beta z}H(t - z/c) \tag{20}$$

with $\hat{\mathbf{s}}$ dependent only on the polar angle θ, and the boundary conditions being $I_d(z = 0, \cos\theta > 0, t) = 0$ and $I_d(z = L, \cos\theta < 0, t) = 0$.

Two cases of incident radiation profiles were considered for comparison with solutions reported in literature.

Continuous collimated pulse

The first case is a continuous collimated pulse corresponding to $I_i(t) = 0, t < 0$ and $I_i(t) = 1.0$ $W/m^2sr, t \geq 0$. A converged solution was reached for a spatial discretization of $N_z = 101$

points and an angular discretization of $N_\theta = 25$ directions. The time interval Δt is equal to $\Delta z/c$ where $\Delta z = L/100$. The CPU time taken was about 6 seconds on a Pentium 4, 2.80 GHz machine for 360 time steps. Figure 5 compares the radiative heat fluxes obtained with the present technique with those obtained by (i) Tan and Hsu [22] using the integral solution and by (ii) Chai [25], using the finite volume technique with the CLAM scheme and the present technique. As can be seen, the modified method of characteristics captures the sharp discontinuities better than the finite volume technique. It should also be noted that Chai [25] used 300 control volumes and 20×1 angles per quadrant equivalent to $N_\theta = 40$ angles for θ varying from 0 to π compared to 101 nodes and $N_\theta = 25$ in the present study.

Ultra-short collimated pulse

The second incident radiation profile is a truncated Gaussian distribution with a peak intensity at $t = t_c$ and pulse width t_p expressed as

$$I_i(t) = I_0 \exp\left[-4\ln(2)\left(\frac{t-t_c}{t_p}\right)^2\right], \qquad 0 < t < 2t_c \tag{21}$$

$$I_i(t) = 0 \qquad t \geq 2t_c \tag{22}$$

Numerical convergence was achieved with a discretization of $N_z = 101$ and $N_\theta = 25$ for the case of $\tau_L = 0.5$ and $N_z = 201$ and $N_\theta = 25$ for the case of $\tau_L = 5.0$. The time interval Δt had little effect on the numerical results as long as $\Delta t \leq \Delta z/c$. Thus, it was set equal to $\Delta z/c$ where $\Delta z = L/(N_z - 1)$ and N_z is the number of gridpoints in the $z-$direction. After solving for the intensities in all directions at every grid point, the hemispherical reflectance $R(t)$ and transmittance $T(t)$ are computed using the following formulae,

$$R(t) = -2\pi \int_{-1}^{0} I_d(0, \mu, t)\mu \mathrm{d}\mu / I_0 \tag{23}$$

and

$$T(t) = [2\pi \int_0^1 I_d(L, \mu, t)\mu \mathrm{d}\mu + I_i(t - L/c)e^{-\beta L} H(t - L/c)]/I_0 \tag{24}$$

The integrals in the formulae for hemispherical reflectance and transmittance are computed using the 3/8 Simpson numerical rule. The CPU time taken for computing the transmittance for the case of $\tau_L = 5.0$ and $\omega = 1.0$ using a spatial discretization of $N_z = 201$ points and an angular discretization of $N_\theta = 25$ was about 41 seconds for a total dimensionless time $t^* = 40$ defined by $t^* = \beta ct$. The CPU time taken for computing the reflectance for the case of $\tau_L = 0.5$ and $\omega = 0.95$ using a spatial discretization of $N_z = 101$ points and an angular discretization of $N_\theta = 25$ directions per octant was about 21 seconds for a total dimensionless time of $t^* = 8$.

Figures 6 and 7 compare the transmittance and reflectance of homogeneous absorbing and isotropically scattering slabs obtained by Wu [20] from the numerical solution of the integral equation with those obtained with the modified method of characteristics. Figure 6 corresponds to the temporal transmittance of a slab of optical thickness $\tau_L = 5.0$ and scattering albedos $\omega = 1.0$ and $\omega = 0.5$. Figure 7 corresponds to the reflectance from a slab of optical thickness $\tau = 0.5$ and scattering albedos of $\omega = 0.95$ and $\omega = 0.5$. Good agreement is observed for both the transmittance and reflectance, and the mean error was less than 5% in all cases. Thus the modified method of characteristics can be used to simulate transport of collimated radiation in a fast and accurate manner. It can be seen from Figure 6 that the temporal distribution of transmittance has two local maxima for large values of the scattering albedo ($\omega = 1.0$). The first peak occurs as soon as the direct pulse or the unscattered radiation reaches the other end of the slab. The second peak is due to the

scattered radiation and so appears only in media where the scattering albedo is large. In media where the scattering albedo is not as large, the contribution to the transmittance from scattering is not large enough to produce a second peak [20]. The reflectance on the other hand depends only on the back-scattered radiation and so has only one peak (see Figure 7) while the peak corresponding to the direct pulse or unscattered radiation is absent unlike the plot of the transmittance. Figure 7 also shows that there is a cusp in the reflectance and occurs at about the same time for both values of scattering albedo. This cusp appears as there is no medium to back-scatter the radiation once the pulse reaches the other end of the slab. It occurs at about the time it takes for the peak of the pulse to travel back and forth between the two faces of the slab. Since the peak occurs at $t = 3t_p$ and it takes $2L/c$ time to travel from one end of the medium and return, the total time taken is $3t_p + 2L/c$ or in dimensionless form, $3\beta c t_p + 2\tau_L = 1.45$ as shown in Figure 7.

4 Discussion

The results presented confirm the validity of the numerical scheme and its capability in handling various transient problems. It has been shown that the modified method of characteristics is a fast and accurate technique to simulate transient radiative transfer in absorbing and scattering media. It can also be easily modified to handle various other geometries and phase functions, thus enabling it to simulate radiative transfer in more complex situations such as those for biomedical applications. The computer program used to implement the described method has not been optimized neither has a thorough error and stability analysis been done. Instead, the study has been aimed at demonstrating the applicability of the

method to a range of problems encountered in transient radiation transfer. A careful study of the errors introduced due to the Lagrangian interpolation should be performed. This would be helpful in comparing the accuracy of this method to other methods like the finite volume method which is prone to false scattering [26]. Also, various improvements can be made to decrease the computational time:

- The number of discrete directions can be reduced or replaced by quadrature as commonly used in the discrete ordinate method to accelerate the computation of the in-scattering term. For example, in situations which involve strong forward scattering, a quadrature with more angles in the forward direction compared to other directions can be made use of thus making the scheme more efficient. This has not been done here for the sake of accuracy, but could be easily implemented.

- To further accelerate the computations, the radiation wavefront can be tracked and computations be performed only at points through which the wave has passed.

- Though the case of a diffusely reflecting boundary condition was not discussed here, it can be easily implemented as done by Rukolaine *et al.* [41]. Also, specularly reflecting boundaries using the modified method of characteristics have been successfully implemented recently for phonon transport [38]. A similar treatment can be applied to partially reflecting and transmitting boundaries.

- Also, since the method is fully explicit it can be easily adapted for parallel computing. This could be a useful feature in inverse problems for biomedical diagnostics or other remote sensing applications.

5 Concluding Remark

The modified method of characteristics has been presented as a scheme for solving the radiative transport equation. It has been shown that the method can handle various problems including multidimensional, transient radiative transport in media exposed to both collimated or diffuse irradiation. The method is fast and accurate and compares well with those obtained using other methods and reported in literature. In particular, the method was able to capture the sharp spatial discontinuities associated with transient radiative transport. Also, since the method makes use of any arbitrary fixed grid, it can be coupled easily with other methods to solve simultaneously occurring transport phenomena like in the case of short-pulse laser heating of metals [39].

Acknowledgements

The authors are thankful to Professor Pei-feng Hsu and Professor John Chai for providing data for the integral equation solution and the finite volume solution.

References

[1] M. F. Modest, *Radiative Heat Transfer*, Academic Press, San Diego, CA, 2002.

[2] S. Kumar and K. Mitra, "Microscale aspects of thermal radiation transport and laser applications", *Advances in Heat Transfer*, vol. 33, pp. 187–294, 1999.

[3] Y. Yamada, "Light-tissue interaction and optical imaging in biomedicine", *Annual Review of Heat Transfer*, vol. 6, no. 2, pp. 1–59, 1995.

[4] K. Mitra and S. Kumar, "Development and comparison of models for light-pulse transport through scattering-absorbing media", *Applied Optics*, vol. 38, no. 1, pp. 188–196, 1999.

[5] Akira Ishimaru, "Diffusion of light in turbid material", *Applied Optics*, vol. 28, no. 12, pp. 2210–2215, 1989.

[6] M.S. Patterson, B. Chance, and B.C. Wilson, "Time resolved reflectance and transmittance for the non-invasive measurement of tissue optical properties", *Applied Optics*, vol. 28, no. 12, pp. 2331–2336, 1989.

[7] R. Elaloufi, R. Carminati, and J. J. Greffet, "Time-dependent transport through scattering media: from radiative transfer to diffusion", *Journal of Optics A: Pure And Applied Optics*, vol. 4, no. 5, pp. S103–S108, 2002.

[8] Z. Guo and K. Kim, "Ultrafast-laser-radiation transfer in heterogeneous tissues with the discrete-ordinates method", *Applied Optics*, vol. 42, pp. 2897–2905, 2003.

[9] Z. Guo, S. Kumar, and K.-C. San, "Multidimensional Monte Carlo simulation of short-pulse transport in scattering media", *Journal of Thermophysics and Heat Transfer*, vol. 14, no. 4, pp. 504–511, 2000.

[10] B. C. Wilson and G. Adam, "A Monte Carlo model for the absorption and flux distributions of light in tissue", *Medical Physics*, vol. 10, no. 6, pp. 824–830, 1983.

[11] S. L. Jacques, "Time resolved propagation of ultrashort laser pulses within turbid tissues", *Applied Optics*, vol. 28, no. 12, pp. 2223–2229, 1989.

[12] Z. Guo and S. Kumar, "Discrete ordinates solution of short pulse laser transport in two-dimensional turbid media", *Applied Optics*, vol. 40, no. 19, pp. 3156–3163, 2001.

[13] M. F. Modest, "Backward Monte Carlo simulations in radiative heat transfer", *ASME Journal of Heat Transfer*, vol. 125, pp. 57–62, 2003.

[14] X. Lu and P.-F. Hsu, "Reverse Monte Carlo method for transient radiative transfer in participating media", *Journal of Heat Transfer*, vol. 126, no. 4, pp. 621–627, 2004.

[15] G. C. Pomraning, *The Equations of Radiation Hydrodynamics*, Pergamon Press, New York, NY, 1973.

[16] A. Munier, "Integral form of the time-dependent radiation transfer equation - I. Inhomogeneous slabs", *Journal of Quantitative Spectroscopy and Radiative Transfer*, vol. 38, pp. 447–455, 1987.

[17] A. Munier, "Integral form of the time-dependent radiation transfer equation - II. Inhomogeneous spherical media", *Journal of Quantitative Spectroscopy and Radiative Transfer*, vol. 38, pp. 457–474, 1987.

[18] A. Munier, "Integral form of the time-dependent radiation transfer equation - III. Moving boundaries", *Journal of Quantitative Spectroscopy and Radiative Transfer*, vol. 38, pp. 475–487, 1987.

[19] A. Munier, "Integral form of the 3-D time-dependent radiation transfer equation in Cartesian coordinates", *Journal of Quantitative Spectroscopy and Radiative Transfer*, vol. 39, pp. 43–48, 1988.

[20] C-Y. Wu, "Propagation of scattered radiation in a participating planar medium with pulse irradiation", *Journal of Quantitative Spectroscopy and Radiative Transfer*, vol. 64, no. 5, pp. 537–548, 2000.

[21] C-Y. Wu and S-H Wu, "Integral equation formulation for transient radiative transfer in an anisotropically scattering medium", *International Journal of Heat and Mass Transfer*, vol. 43, no. 11, pp. 2009–2020, 2000.

[22] Z.-M. Tan and P.-F. Hsu, "An integral formulation of transient radiative transfer", *ASME Journal of Heat Transfer*, vol. 123, pp. 466–475, 2001.

[23] Z.-M. Tan and P.-F. Hsu, "Transient radiative transfer in three-dimensional homogeneous and non-homogeneous participating media", *Journal of Quantitative Spectroscopy and Radiative Transfer*, vol. 73, pp. 181–194, 2002.

[24] G. D. Raithby and E. H. Chui, "A finite-volume method for predicting a radiant heat transfer in enclosures with participating media", *Journal of Heat Transfer*, vol. 112, pp. 415–423, 1990.

[25] J.C. Chai, "One-dimensional transient radiation heat transfer modeling using a finite-volume method", *Numerical Heat Transfer, Part B*, vol. 44, pp. 187–208, 2003.

[26] J. C. Chai, P.-F. Hsu, and Y.C. Lam, "Three-dimensional transient radiative transfer modeling using the finite-volume method", *Journal of Quantitative Spectroscopy and Radiative Transfer*, vol. 86, pp. 299–313, 2004.

[27] Z. Guo and S. Kumar, "Radiation element method for transient hyperbolic radiative transfer in plane parallel inhomogenous media", *Numerical Heat Transfer,Part B*, vol. 39, no. 4, pp. 371–387, 2001.

[28] M. Sakami, K. Mitra, and P.-F. Hsu, "Analysis of light pulse transport through two-dimensional scattering and absorbing media", *Journal of Quantitative Spectroscopy and Radiative Transfer*, vol. 73, pp. 169–179, 2002.

[29] Z. Guo and S. Kumar, "Three-dimensional discrete ordinates method in transient radiative transfer", *Journal of Thermophysics and Heat Transfer*, vol. 16, no. 3, pp. 289–296, 2002.

[30] H. Quan and Z. Guo, "Fast 3-D optical imaging with transient fluorescence signals", *Optics Express*, vol. 12, no. 3, pp. 449–457, 2004.

[31] J. D. Hoffman, *Numerical Methods for Engineers and Scientists*, McGraw Hill, New York, NY, 1998.

[32] A. Allievi and R. Bermejo, "Finite element modifed method of characteristics for Navier-Stokes equations", *International Journal for Numerical Methods in Fluids*, vol. 32, no. 4, pp. 439–464, 2000.

[33] D. L. Marcum and J. D. Hoffman, "Calculation of three-dimensional flowfields by the unsteady method of characteristics", *AIAA Journal*, vol. 23, no. 10, pp. 1497–1505, 1965.

[34] B. N. Wang and J. D. Hoffman, "Calculation of annular nozzle trisonic flowfields by the method of characteristics", *Journal of Propulsion and Power*, vol. 4, no. 3, pp. 228–235, 1987.

[35] L. Pilon and R. Viskanta, "Modified method of characteristics for solving the population balance equation", *International Journal for Numerical Methods in Fluids*, vol. 42, pp. 1211–1236, 2003.

[36] L. Pilon, A. G. Fedorov, D. Ramkrishna, and R. Viskanta, "Bubble transport in three-dimensional gravity driven flow, part i. mathematical formulation", *Journal of Non-Crystalline Solids*, vol. 336, pp. 71–83, 2004.

[37] L. Pilon and R. Viskanta, "Bubble transport in three-dimensional gravity driven flow, part ii. numerical results", *Journal of Non-Crystalline Solids*, vol. 336, pp. 84–95, 2004.

[38] L. Pilon and K. Katika, "Backward method of characteristics for simulating microscale energy transport", *in ASME Journal of Heat Transfer*, vol. 126, pp. 735–743, 2004.

[39] T. Q. Qiu and C. L. Tien, "Short pulse laser heating in metals", *International Journal of Heat and Mass Transfer*, vol. 35, pp. 719–726, 1992.

[40] P. J. Coelho, "Bounded skew high-order resolution schemes for the discrete ordinates method", *Journal of Computational Physics*, vol. 175, no. 2, pp. 412–437, 2002.

[41] S. A. Rukolaine, M . G. Vasilyev, V. S. Yuferev, and A. O. Galyukov, "Numerical solution of axisymmetric radiative heat transfer problems in arbitrary domains using the characteristic method", *Journal of Quantitative Spectroscopic and Radiative Transfer*, vol. 73, pp. 205–217, 2002.

FIGURE AND TABLE CAPTIONS

Figure 1. Typical computational cell used for inverse marching method containing the pathline of the photons.

Figure 2. Block diagram of the numerical procedure for solving the RTE by the modified method of characteristics.

Figure 3. Radiative flux distribution at different times in a 1-D homogeneous medium with a diffusely emitting boundary.

Figure 4. Radiative flux distribution at different times in a 3-D homogeneous medium with a diffusely emitting boundary for $\tau = 1.0$ and $\omega = 0.1$ using different techniques.

Figure 5. Radiative flux distribution at different times in a 1-D homogeneous medium exposed to continuous collimated irradiation.

Figure 6. Time-resolved hemispherical transmittance for $\tau_L = 5.0$, $t_c/t_p = 3$ and $\beta c t_p = 0.33$.

Figure 7. Time-resolved hemispherical reflectance for $\tau_L = 0.5$, $t_c/t_p = 3$ and $\beta c t_p = 0.15$.

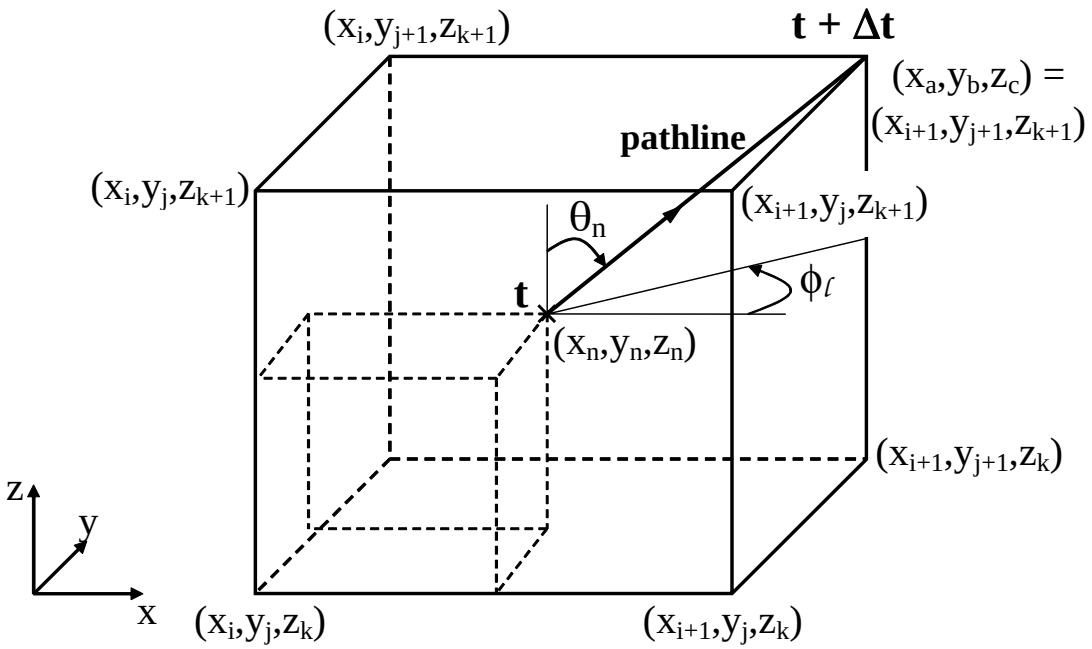

Figure 1: Typical computational cell used for inverse marching method containing the path-line of the photons.

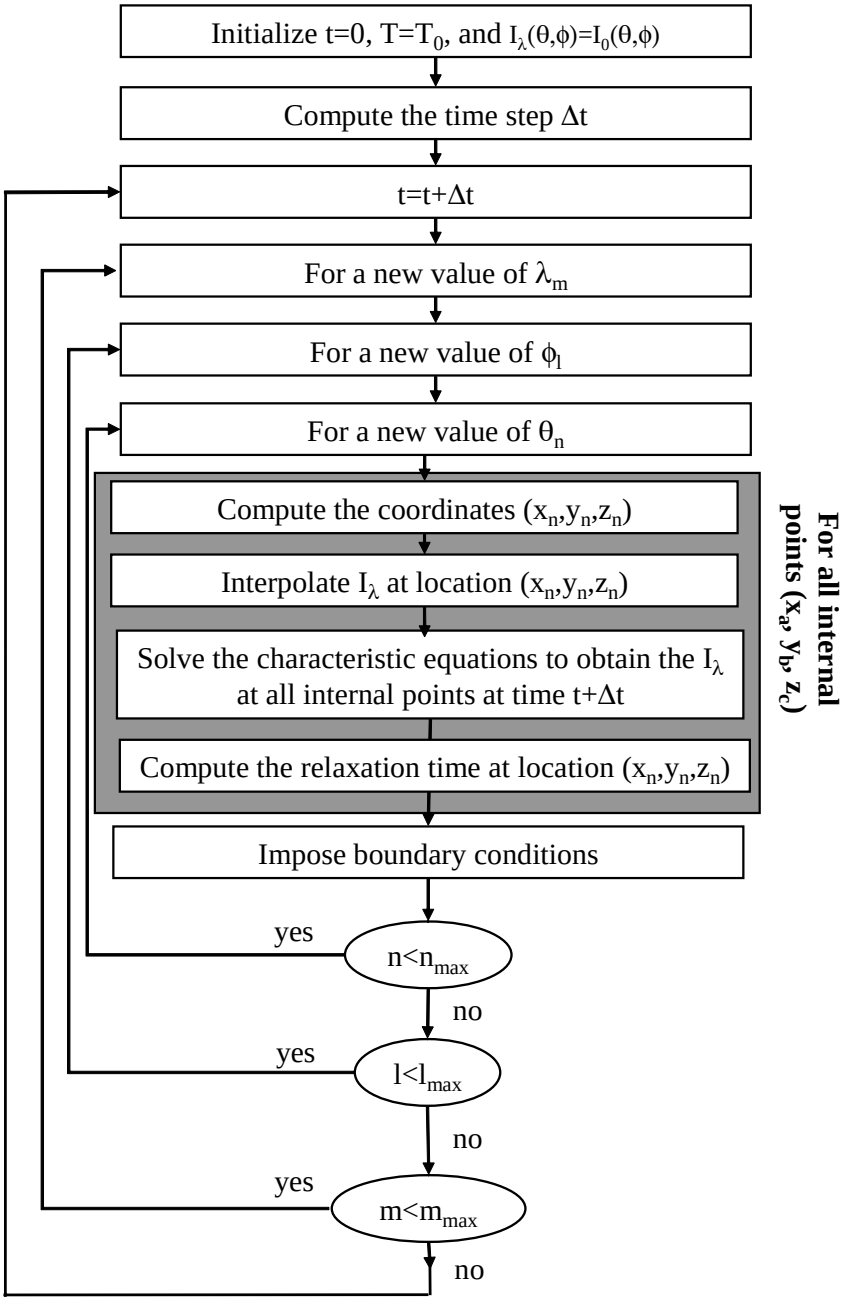

Figure 2: Block diagram of the numerical procedure for solving the RTE by the modified method of characteristics.

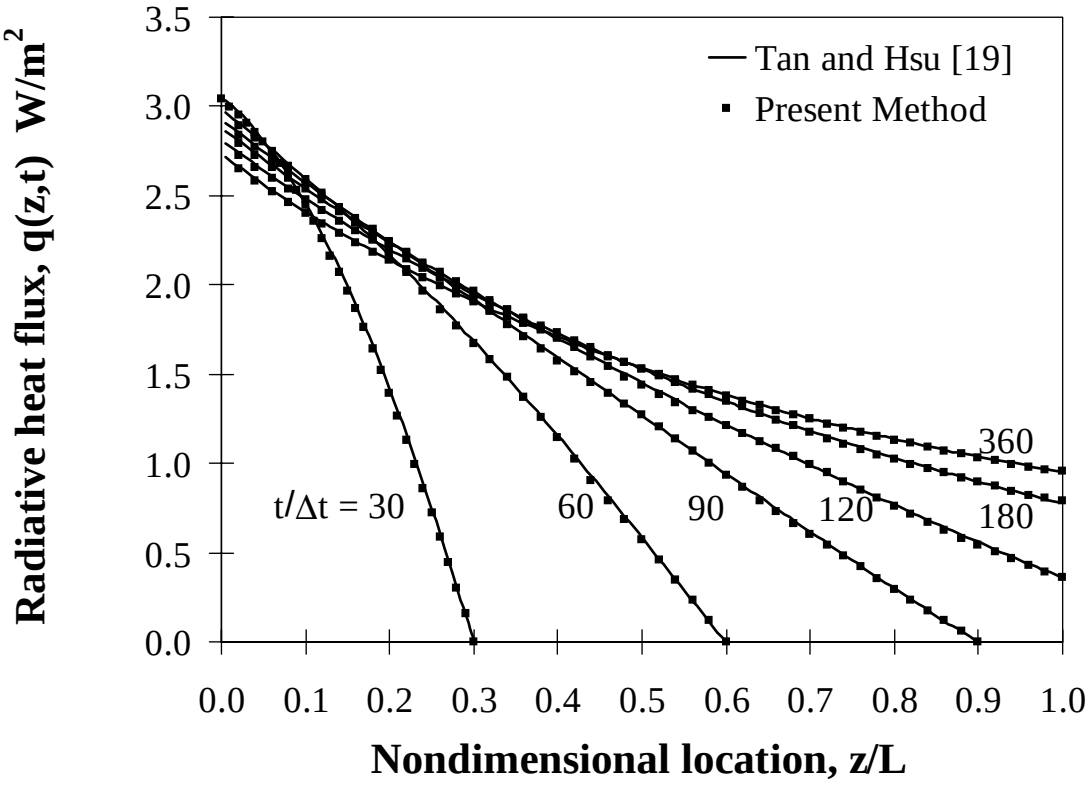

Figure 3: Radiative heat flux distribution at different times in a 1-D homogeneous medium with a diffusely emitting boundary.

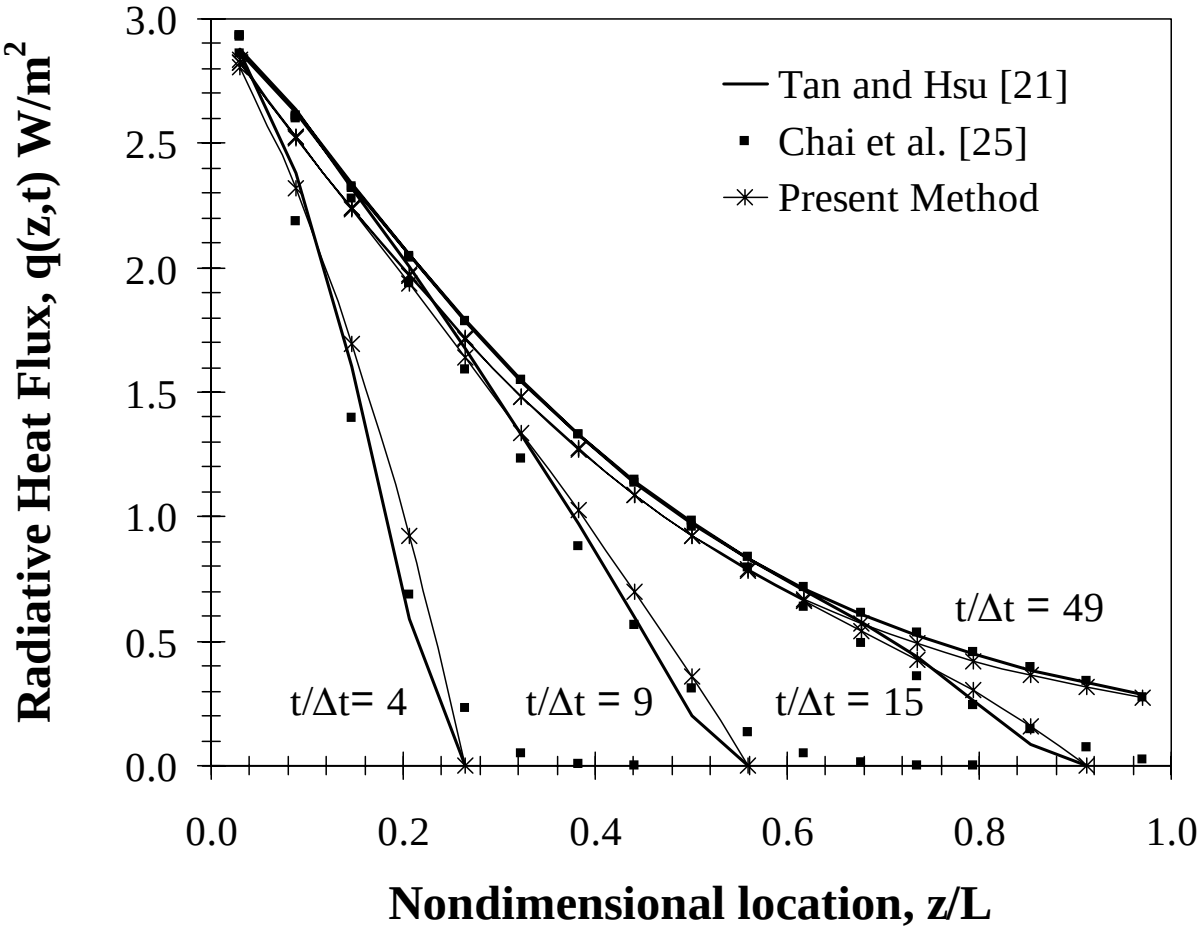

Figure 4: Radiative heat flux distribution at different times in a homogeneous 3-D medium with a diffusely emitting boundary for $\tau = 1.0$ and $\omega = 0.1$.

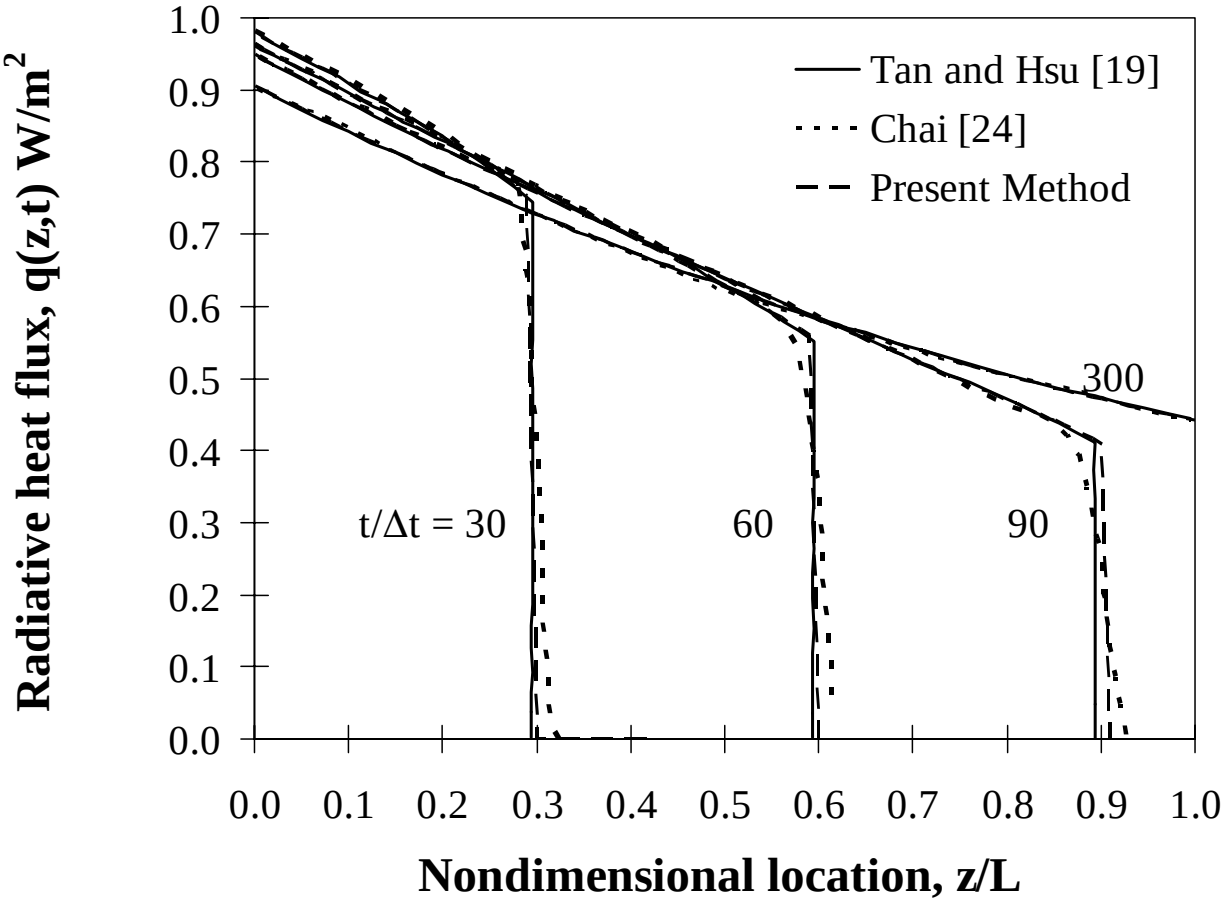

Figure 5: Radiative flux distribution at different times in a 1-D homogeneous medium exposed to continuous collimated irradiation.

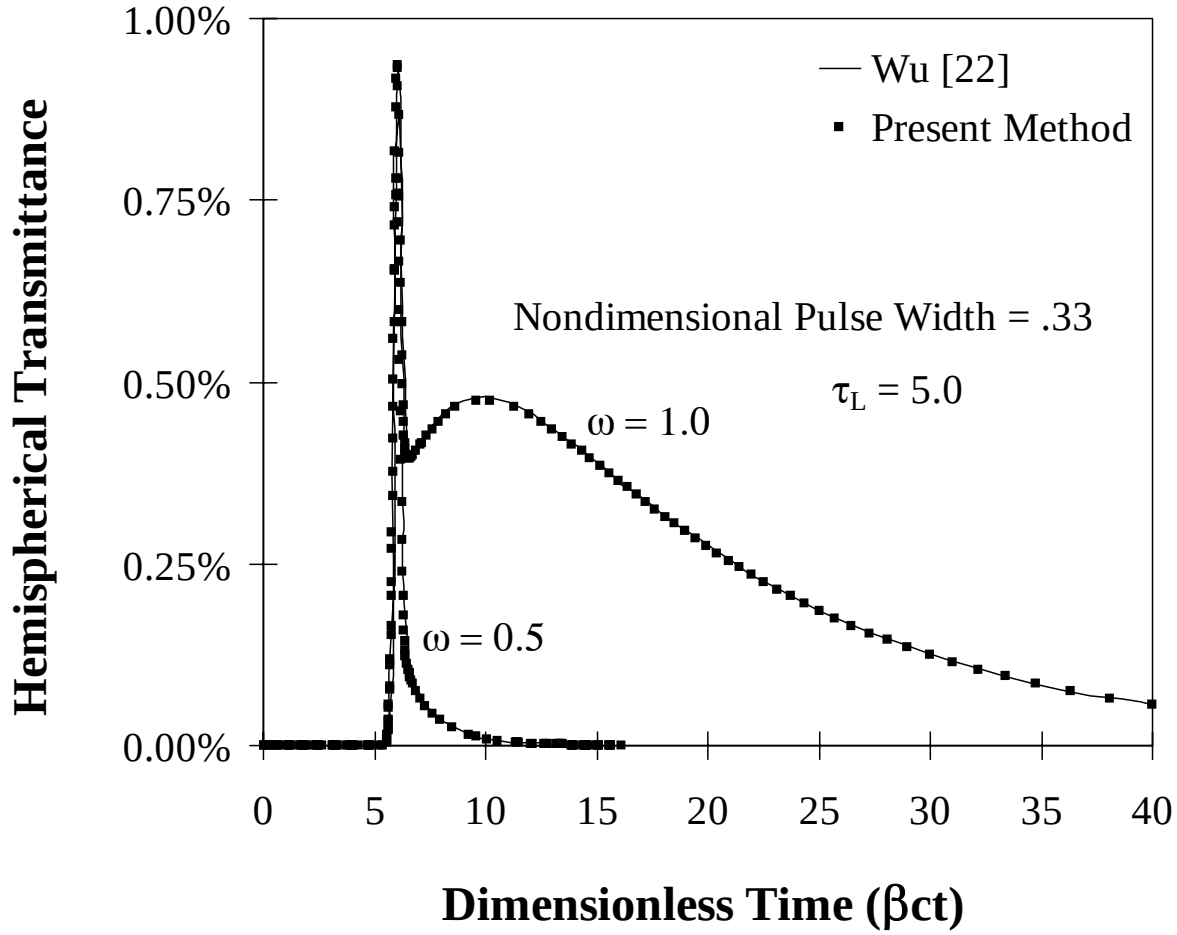

Figure 6: Time-resolved hemispherical transmittance for $\tau_L = 5.0$, $t_c/t_p = 3$ and $\beta c t_p = 0.33$

.

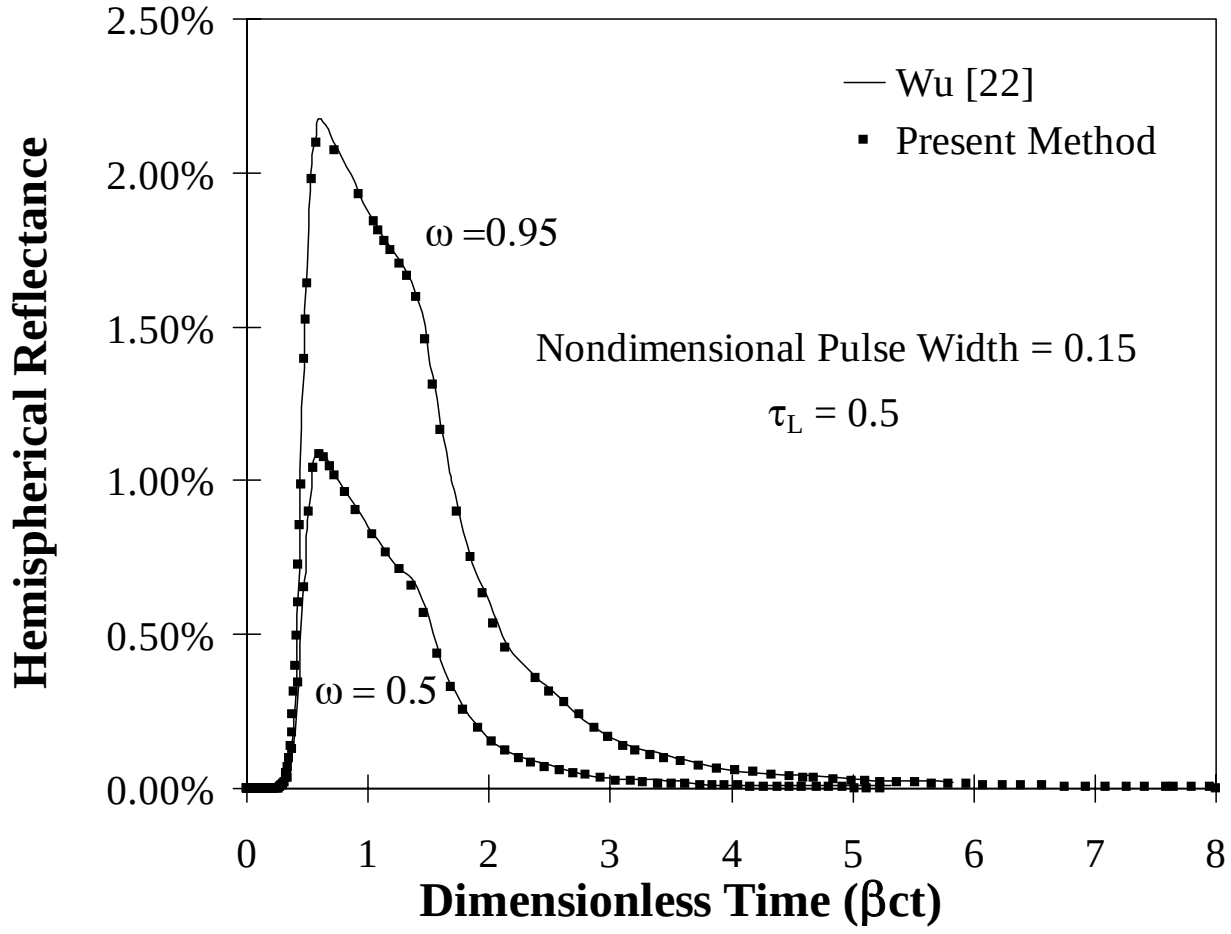

Figure 7: Time-resolved hemispherical reflectance for $\tau_L = 0.5$, $t_c/t_p = 3$ and $\beta c t_p = 0.15$.